

Article

1 **Identifying and protecting macroalgae detritus sinks toward climate change mitigation**

2 Ana M Queirós¹, Karen Tait¹, James R Clark¹, Michel Bedington¹, Christine Pascoe¹,

3 Ricardo Torres¹, Paul J Somerfield¹ and Dan A Smale²

4 ¹Plymouth Marine Laboratory, Devon, UK

5 ²Marine Biological Association of the United Kingdom, Devon, UK

6 **Corresponding Author:** Ana M Queirós anqu@pml.ac.uk;

7

8 Open Research: Experimental data produced during this study is publicly archived and
9 accessible in Queirós, A. M. and C. Pascoe (2020). Mesocombs investigation of seaweed
10 fragment degradation and skinking rates. Zenodo. doi:10.5281/zenodo.4309608.

11 All field eDNA sequence data is publicly available for download at the NCBI SRA database,
12 using the BioProject number PRJNA472452 (Eukaryote diversity assessment of sediments of
13 the Western English Channel).

14 Code for models FVCOM and PyLag used here has been previously published.

15

16 **Abstract**

17 Harnessing natural solutions to mitigate climate change requires an understanding of carbon
18 fixation, flux and sequestration across ocean habitats. Recent studies suggest that exported
19 seaweed particulate organic carbon is stored within soft sediment systems. However, very
20 little is known about how seaweed detritus disperses from coastlines, or where it may enter
21 seabed carbon stores, where it could become the target of conservation efforts. Here, focusing
22 on regionally dominant seaweed species, we surveyed environmental DNA (eDNA) of
23 natural coastal sediments, and studied their connectivity to seaweed habitats using a particle
24 tracking model parameterized to reproduce seaweed detritus dispersal behavior based on
25 laboratory observation of seaweed fragment degradation and sinking. Experiments showed

Article

26 seaweed detritus density changing over time, differently across species. This, in turn,
27 modified distances travelled by released fragments until they reached the seabed for the first
28 time, during model simulations. Dispersal pathways connected detritus from the shore to the
29 open ocean but, importantly, also to coastal sediments, and this was reflected by field eDNA
30 evidence. Dispersion pathways were also affected by hydrodynamic conditions, varying in
31 space and time. Both the properties and timing of released detritus, individual to each
32 macroalgal population, and short-term near-seabed and medium-term water-column transport
33 pathways, are thus seemingly important in determining the connectivity between seaweed
34 habitats and potential sedimentary sinks. Studies such as this one, supported by further field
35 verification of sedimentary carbon sequestration rates and source partitioning, are still needed
36 to help quantify the role of seaweed in the ocean carbon cycle. Such studies will provide vital
37 evidence to inform on the potential need to develop blue carbon conservation mechanisms,
38 beyond wetlands.

39 **Keywords:** blue carbon, climate change, conservation, lagrangian, mitigation, seaweed.

41 **Introduction**

42 The short time-frame required to limit global greenhouse gas emissions to avoid planet-
43 altering climate change has injected momentum into efforts to expand the contribution of
44 ocean-based solutions within Nationally Determined Contributions to the Paris
45 Agreement (Gallo, Victor, and Levin 2017; Hoegh-Guldberg et al. 2019). “Blue carbon”
46 describes natural carbon sequestration in the ocean. Historically, the term has referred to
47 vegetated coastal habitats including mangroves, seagrass beds and salt marshes, where carbon
48 is fixed as part of a stable living biomass store, and organic matter trapped within sediments
49 provides long-term storage. Blue carbon activities are thus management activities that protect
50 these habitats (and associated carbon stores) from disturbance, supporting climate change

Article

51 mitigation through the resulting regulation of CO₂ (and potentially other greenhouse gas)
52 emissions(Mcleod et al. 2011; Herr, Pidgeon, and Laffoley 2012). However, recent work has
53 highlighted that vegetated coastal habitats represent a small fraction of coastal and marine
54 ecosystems that contribute to blue carbon(Krause-Jensen et al. 2018; Queirós et al. 2019;
55 Raven 2018). In contrast, seaweed-dominated habitats are distributed across almost a third of
56 global coastlines and are amongst the most productive vegetated habitats globally(Smith
57 1981; Feehan, Filbee-Dexter, and Wernberg 2021). This production is not yet considered
58 within global carbon budgets, as seaweed are typically not represented within global ocean
59 biogeochemistry models (Friedlingstein et al. 2020). This indicates that there is currently a
60 potential blind spot in our global assessment of the ocean as a potential carbon sink. Seaweed
61 habitats are also not typically considered within blue carbon activities because they are
62 overwhelmingly found on rocky shorelines and reefs, where there is limited potential for *in-*
63 *situ* storage of the organic carbon they produce(Krause-Jensen et al. 2018).

64 For kelp (a dominant seaweed group), it has been estimated >80 % of annual production is
65 exported from source habitats(Krause-Jensen and Duarte 2016), with export rates in some
66 systems exceeding 95%(Smale et al. *in press*). A recent global study argued that this exported
67 production, estimated at 323 Tg C/yr¹⁰, may be globally available across the ocean water
68 column(Ortega et al. 2019). The fate of this exported carbon is very poorly understood, but
69 the inclusion of seaweed in blue carbon activities requires the verification that its carbon is
70 sequestered in the long-term, in a way that is amenable to management(Sutton-Grier and
71 Howard 2018). So although such a blue carbon scheme already exists (e.g. Yokohama Bay
72 seaweed farming (Kuwae et al. 2022)) very few studies have heretofore measured the
73 contribution of seaweed carbon to sedimentary carbon stores in the wild. One study provided
74 evidence that 4-9% of the annual production of wild seaweed is sequestered as particulate
75 organic carbon (POC) in coastal non-vegetated sediments (i.e. soft-sediment beds), that is,

Article

76 outside of those typically considered within the blue carbon umbrella(Queirós et al. 2019).
77 Other studies have not yet measured seaweed POC sedimentary sequestration rates, but have
78 used environmental DNA (eDNA) alone to suggest that this may be taking place both inside
79 and outside of vegetated habitats(Ortega et al. 2019; Ortega, Geraldi, and Duarte 2020).
80 Another measured farmed seaweed contribution to the ocean's recalcitrant dissolved organic
81 carbon pool(Li et al. 2022). These novel findings lend weight to the notion that seaweed may
82 be an important component of blue carbon that is amenable to management, once habitats
83 serving as sinks for this exported production can be identified(Polis, Anderson, and Holt
84 1997; Smale et al. 2018; Hunt 1925; Queirós et al. 2019). However, large questions still
85 remain regarding how general the findings from these studies(Queirós et al. 2019; Ortega et
86 al. 2019; Ortega, Geraldi, and Duarte 2020) may be, and therefore about the role of seaweed
87 carbon within the context of long-term carbon sequestration(Sutton-Grier and Howard 2018).
88 In particular, large uncertainties remain around: the fate of seaweed POC that is released as
89 macroalgal detritus; what fraction of this remains in, and is potentially sequestered within, the
90 coastal ocean (cf. exported to the open ocean and deep sea areas); as well as around the
91 ability to identify and quantify the transport pathways that connect carbon source to sink
92 habitats(Queirós et al. 2019; Smale et al. 2018). Without this knowledge, we cannot manage
93 donor and sink habitats jointly, conserve them, or restore them. Improved management of
94 seaweed-derived carbon, as well as growing investment in seaweed farming, are seen as vital
95 approaches to curbing global carbon emissions². However, regardless of the high productivity
96 of seaweed habitats, understanding connectivity and identifying their associated sink habitats
97 is a pre-requisite for conserving and promoting sequestration of their carbon(Bianchi et al.
98 2018; Li et al. 2022).
99 To this end, improved understanding of a number of additional processes operating at the
100 sediment-water interface; a significant expansion of existing field-based data; and the

Article

101 development and application of appropriately parameterized dispersal models that may
102 enable the identification of detritus sink locations are needed, among other
103 innovations(Queirós et al. 2019; Krause-Jensen and Duarte 2016; Krause-Jensen et al. 2018).
104 Here, we contribute to the delivery of these aims, by investigating the following questions: i)
105 how widely distributed is seaweed detritus in coastal sediments?; ii) how does seaweed
106 detritus degradation impact transport dynamics and fate?; and iii) what transport pathways
107 connect seaweed habitats to putative carbon sink habitats in the coastal ocean, and how
108 dynamic are these? A two-year study combined novel field observations of environmental
109 DNA, as well as, to our knowledge, the first application of Lagrangian particle tracking
110 modeling using parameter values estimated via lab-based observations of seaweed detritus
111 degradation and sinking velocity. We focused on the coastal ocean, where the largest fraction
112 of seaweed detritus is expected to remain(Krause-Jensen and Duarte 2016), and where the
113 majority of the world's MPAs are already located(UNEP-WCMC and IUCN 2020) with
114 conservation mechanisms more easily implemented.

115

116 **Methods**117 *Sedimentary eDNA sampling and processing*

118 To address our first research question, we sampled marine soft-sediments at two inshore
119 coastal areas in Plymouth Sound UK (one *Zostera marina* seagrass meadow and one non-
120 vegetated) and one offshore site, circa 48 m deep and 13 km S-SW off Plymouth, which hosts
121 the benthic site of the long-term monitoring Station L4 (50° 13' 22.7''N 4° 11'23.0''W ,
122 <https://www.westernchannelobservatory.org.uk/>)(Queirós et al. 2019). We analysed
123 sedimentary eDNA sampled from all three areas collected during one common time point,
124 whilst the offshore area was further sampled on another 6 occasions over a 13 month period
125 (Fig. 1; Queirós et al. 2019). Offshore sampling took place as previously described (Queirós

Article

126 et al. 2019), via deployment of a multi-corer (which penetrates between 30-50 cm into
127 sediments depending on sediment type), sediment slicing, and the collection of small volumes
128 of sediment from the preserved sediment water interface (0-2cm), which were frozen in
129 liquid nitrogen on collection and until retrieval to Plymouth Marine Laboratory, where they
130 were stored at -80°C until processing (Queirós et al. 2019). 3-4 eDNA samples were collected
131 at the offshore site at each sampling event, corresponding to one per multi-corer core
132 (Queirós et al. 2019). The seabed at the site is characterised as sandy mud (Queirós,
133 Stephens, et al. 2015); its sediment surface is covered by a bottom water layer of varying
134 thickness (cms) comprised of detritus, fine sediment and living organisms, that is flushed and
135 re-settled tidally (the “fluff layer”, Queirós et al. 2019); and the site is influenced by outflow
136 from the Tamar estuary (Smyth et al. 2015). Inshore sediment samples were collected by
137 scuba divers in April 2016, just before the last offshore sampling campaign (Queirós et al.
138 2019). Triplicate core samples were collected from a shallower area (~2 m depth below chart
139 datum) dense with seagrass shoots (*Zostera marina* (Linnaeus)), and from a deeper
140 unvegetated area (~8 m depth below chart datum) in Firestone Bay, Plymouth, SW UK (Fig
141 1). Firestone Bay is characterized by patches of soft sediment, interspersed within semi-stable
142 boulders and bedrock harboring dense macroalgal assemblages (De Leij et al. 2017). Seagrass
143 shoot density in the sampled area was circa ~60 m⁻² at the shallower site, whereas the deeper
144 sampling area was characterized by fine sediments supporting abundant infauna. Firestone
145 Bay is also influenced by tidal currents and riverine input from the nearby Tamar Estuary;
146 however, its waters are considered well-mixed and fully marine (Smyth et al. 2015). Divers
147 collected surficial sediment cores using sterile piston corers made from cut-off 60 mL
148 polyethylene syringes (2.9 cm diameter). Syringes were inserted vertically 8 cm into the
149 sediment, capped, and returned to the laboratory where they were frozen at -80°C until later
150 analysis. Care was taken not to disturb the sediment layer before sampling and to retain

Article

151 sediments on retrieval of syringes. Three replicate core samples were collected haphazardly
152 within each area, from locations positioned at least 3 m apart from one another. From each
153 syringe core, samples were extracted from the surficial 2 cm sediment for eDNA analysis, as
154 done for offshore samples, with inshore and offshore samples compared in subsequent
155 analyses.

156 eDNA was extracted from all sediment samples using the MoBIO Powersoil DNA©
157 extraction kit following the manufacturer's guidelines. The V9 region of the 18S rRNA gene
158 was amplified using the primer pair Euk1391F (GTACACACCGCCCGTC) and EukBr
159 (TGATCCTTCTGCAGGTTACCTAC) (Amaral-Zettler et al. 2009), and sequenced using
160 MiSeq by commercial contract (Mr DNA, Molecular Research LP, USA). Distinct
161 Operational Taxonomic Units' (OTU) sequences were then allocated to taxa at the lowest
162 possible taxonomic resolution using the Basic Local Alignment Search Tool (BLAST) of the
163 National Centre for Biotechnology Information (NCBI, U.S. National Library of Medicine),
164 and then individually quality controlled. All sequences, including those from the offshore site
165 preliminarily analyzed in (Queirós et al. 2019), were re-analyzed in October 2020 to capture
166 the most up-to-date DNA sequence library data. Only sequences which closely matched
167 Chlorophyta, Rhodophyta and Ochrophyta seaweeds were included in our analyses. The
168 resulting eDNA presence-absence data for individual seaweed taxa (lowest level possible) in
169 sediments was analyzed in PRIMER 7.0 (PRIMER-E Ltd, Plymouth, UK). Bray-Curtis
170 similarity of presence-absence taxa data was estimated and visualized using Non-metric
171 Multi-Dimensional Scaling (nMDS) plots. Two way-PERMANOVA (Anderson 2014) was
172 then used to test for differences in the taxonomic composition of the sedimentary eDNA pool
173 between sites (inshore and offshore) and over time (offshore site only), using 999
174 permutations. Pair-wise comparisons between any identified groups were assessed using
175 permutational pseudo-t-tests.

Article

176 *Laboratory estimation of macroalgae detritus degradation and sinking rates*

177 To address our second research question, we investigated how the physical properties of
178 degrading seaweed fragments that affect their transport in the wild change over time, upon
179 release from source, and specifically, fragment buoyancy. Four species of macroalgae widely
180 abundant in the shores surrounding Plymouth Sound, and known to contribute to particulate
181 detritus identified at the offshore area sediments(Queirós et al. 2019), were sampled in
182 September 2017 at low water, by hand, from the shore at Rame Head, Plymouth Sound
183 (50°18' 41.9" N 4°13' 15.9" W) via snorkeling. The species sampled were: *Himanthalia*
184 *elongata* (Linnaeus; Phaeophyceae), *Laminaria digitata* (Hudson; Phaeophyceae),
185 *Saccharina latissima* (Linnaeus; Phaeophyceae), and *Palmaria palmata* (Linnaeus;
186 Floridophyceae). Individuals were immediately returned to the laboratory and held in aerated
187 seawater in the dark, overnight. Unfiltered seawater had been collected at the offshore
188 sampling site on board the RV Quest in the week prior to experiments, and kept in the dark in
189 the PML mesocosm laboratory to avoid autotroph growth, being allowed to adjust to
190 laboratory controlled temperature conditions. On the following day, fragments from central
191 areas of blades of all species and from receptacles (hereafter “straps”) of *H. elongata*
192 (devoid of epibionts) were excised from four individuals of each species. Three fragments
193 were cut perpendicularly to the length of the blades and straps from four individuals across
194 the four species (12 total per species), with lengths 2 cm, 5 cm and 10 cm, respectively. All
195 fragment dimensions were recorded along with fresh weights. Sinking velocities were then
196 estimated in a stationary 35 cm seawater column in the laboratory, using the same seawater
197 sampled at the start of the experiments which had been allowed to settle overnight in a large
198 glass tank. Each fragment was placed parallel to, and on top of, the water surface, and time to
199 reach the bottom of the assessment tank recorded. Sinking velocity was estimated by dividing
200 water column height by time of sinking. The fragments were then distributed across 16 x 8 L

Article

201 seawater aquaria, housing one fragment from each species sampled. Seawater in aquaria was
202 agitated by aquarium pumps of the same make and model across all aquaria, the inlets of
203 which had been covered by a 63 μm mesh to prevent uptake of detritus. All aquaria were held
204 in a seawater bath to minimise temperature differences between aquaria. Bath water was
205 chilled to 16 °C using an aquarium chiller and agitated via aquaria pumps. This baseline
206 temperature was chosen as it reflects the mean temperature experienced by seabed organisms
207 in Plymouth Sound at this time of year (Queirós, Fernandes, et al. 2015). LED blocks
208 (Biolumen, UK) were fitted to a frame positioned at the top of the seawater bath, and the
209 whole setup covered by PVC sheets to reduce evaporation. LED blocks were programmed to
210 mimic the photoperiod of the collection site at the time of experiments. During incubations,
211 seawater temperature in aquaria was 18.01 \pm 2.44 °C (mean \pm SD), pH was 8.26 \pm 0.13,
212 and salinity was 34.09 \pm 0.80 psu. The incubations lasted 35 days, at end of which sinking
213 velocity measurements were repeated. Sinking velocities were analyzed using stepwise linear
214 regression model fitting, based on Akaike's Information Criterion in R (R Core Team 2020)
215 (package "MASS"). We tested for three main effects (experimental day, species and
216 fragment length) as well as their first and second order interactions. Linear model
217 assumptions were verified via graphical analyses of residuals and normal QQ plots, with
218 extreme values with high leverage removed. Residuals were moderately right skewed and so
219 were \log_{10} transformed to meet the normality of residuals assumption of the linear model.

220 *Modelling the transport and dispersal of macroalgal detritus in Plymouth Sound*

221 To address our third research question, we used experimental data to parameterize a transport
222 model to reflect the buoyancy of seaweed fragments in the water column. The modelling of
223 macroalgal detritus transport (and thus dispersal) was achieved via a two-step process. First,
224 a fine-scale hydrodynamic model for the area was configured and run; and variables
225 describing the simulated flow field saved to file every hour. An offline particle tracking

Article

226 model was then used to compute trajectories of initially buoyant detrital particles, based on
227 the outputs of the hydrodynamic model. For this study, we used the Finite Volume
228 Community Ocean Model (FVCOM(Chen, Liu, and Beardsley 2003)), configured for the
229 Plymouth Sound and surrounding coastal area ($\sim 49.7^\circ - 50.6^\circ$ N and $\sim 4.8^\circ - 3.8^\circ$ W,
230 Figure S1). FVCOM is a prognostic, unstructured-grid, finite-volume, free-surface, 3D
231 primitive equation coastal ocean circulation model(Chen, Liu, and Beardsley 2003). Vertical
232 turbulent mixing was modelled with the General Ocean Turbulence Model (GOTM) using a
233 κ - ω formulation(Umlauf and Burchard 2005) whilst horizontal mixing was parameterised
234 using the Smagorinsky scheme(Smagorinsky 1963) with a coefficient of 0.1. The
235 unstructured horizontal grid allows variable resolution across the domain to reflect the
236 complexity of the flow and scale of bathymetric features. The resolution of the model is ~ 600
237 m at Station L4, becoming finer towards the Plymouth Sound (~ 85 m), with highest
238 resolution around the upper River Tamar channel (~ 40 m). The vertical grid is comprised of
239 24 equally spaced layers in terrain following (sigma) coordinates, allowing water column
240 structure in shallower areas to be resolved in fine detail.

241 Atmospheric boundary data, including heat fluxes and surface stresses, were generated by
242 downscaling the National Oceanic and Atmospheric Administration's (NOAA) Global
243 Forecast System model, using a 3 level nested configuration of the Weather Research and
244 Forecasting (WRF(Skamarock et al. 2008)) model, yielding a final resolution of 3 km. River
245 input data was taken from the National River Flow Archive
246 (<http://nrfa.ceh.ac.uk/data/station>). We used river gauge data for 11 rivers within the domain
247 with temperature modelled using a regression model against WRF surface temperatures.

248 Lateral boundary conditions were taken from the Atlantic Margin Model retrieved via the
249 CMEMS service(North West Shelf Monitoring and Forecasting Center 2020), adjusted to the
250 internal tidal solution. FVCOM was run for May 2016, matching the period when eDNA was

Article

251 sampled at all three field sampling sites. The model simulation was extensively validated
 252 against underway ship tracks for this period and against tidal gauge and Acoustic Doppler
 253 Current Profiler measurements for a longer period run using the same setup (see Appendix
 254 S1). The model was shown to reproduce well the Tamar river plume and salinity structure
 255 between the coast and L4 (please refer to the section on model validation in Appendix S1).
 256 Particle tracking simulations were then performed using the offline particle tracking model
 257 PyLag v0.6(Uncles et al. 2020) (<https://github.com/pmlmodelling/pylag>). Particles
 258 were released from two circular release zones with a radius of 10 m and centered on (-4.22°
 259 E, 50.31 ° N) and (-4.14° E, 50.36° N). The two sites are in shallow, near coast waters off
 260 Rame Head and within Plymouth Sound respectively, matching shore communities sampled
 261 during our laboratory investigation into seaweed degradation and eDNA sampling carried out
 262 in this study (Figure 1). All particles were released at the surface, simulating initially
 263 buoyant seaweed detritus. To compute the time it takes initially buoyant particles to reach the
 264 bed once they start sinking through a turbulent water column, a set of simulations were also
 265 performed using input data from the General Ocean Turbulence Model configured for L4
 266 (see Appendix S1).

267 To compute particle trajectories, the particle tracking model solves the equation:

$$268 \quad \frac{\partial}{\partial t} \mathbf{X}_i(t, \mathbf{r}_i) = \mathbf{U}_i(t, \mathbf{X}_i) \quad (1),$$

269 where $\mathbf{r}_i = \mathbf{X}_i(t = t_0)$ is the position vector of particle i at time $t = t_0$, \mathbf{U}_i is the particle's
 270 velocity vector, and $\mathbf{U}_i = [\mathbf{u}(t, \mathbf{x})]_{\mathbf{x} = \mathbf{X}_i}$ in the case of passive transport, where \mathbf{u} is the fluid
 271 velocity vector. The particle velocity vector is broken down into resolved and unresolved
 272 components, which are incorporated into a Random Displacement Model of the form:

$$273 \quad dX_j = \left[u_j + \frac{\partial D_{jk}}{\partial x_k} \right] dt + (2D_{jk})^{1/2} dW_k \quad (2).$$

Article

274 Here, $dX_j = d\mathbf{X}$ is the incremental change in a particle's position and D_{jk} is the diffusion
275 tensor. dW_k is an incremental Wiener process that builds stochasticity into the model.
276 Equation (2) is integrated numerically to compute particle trajectories. Velocity and eddy
277 diffusion terms are linearly interpolated in both space and time to particle positions. To
278 simulate the movement of buoyant particles, a restoring function was used to keep detrital
279 particles at the surface over the course of the simulations. Changes in detrital particle
280 buoyancy over time were not modelled explicitly but are interpreted based on our
281 experimental study. Lastly, the contribution of Stoke's drift was not included explicitly;
282 however, a discussion of its likely impact is included in the discussion section. Further details
283 of the run configuration options used with the particle tracking model are provided in the
284 Appendix S1. Details on model configuration with FVCOM inputs can be found in PyLag's
285 documentation (<https://pylag.readthedocs.io/en/latest/>).
286 To assess the impact of time varying environmental conditions on seaweed detritus transport,
287 two sets of simulations were run. The first set cover a 14 day period starting on 1st May 2016.
288 The period starts with neap tides and a fresh breeze blowing from the south-west and west.
289 After a few days, the wind weakens and switches to come mainly from the east (Appendix
290 S1: Figure S7c). The second set of simulations cover a 14 day period starting on 16th May
291 2016. Again, the period starts with neap tides. However, it is characterized by fresh to strong
292 breezes that predominantly come from the south-west and west (Appendix S1: Figure S7d).
293 In each simulation, 10,000 particles are released from each site at 14 consecutive high waters.
294 Particle simulations were run forward for a total of 14 days each, with particle positions
295 saved to file every 15 minutes. Connectivity between the release sites and the offshore L4
296 benthic sampling site (Fig. 1) was calculated by computing the time of flight to a square of
297 side 2 km centered on L4 benthic (-4.18° E, 50.22° N).

298 **Results**

Article

299 *Macroalgal eDNA in sediments*

300 We identified macroalgal eDNA in all areas and all samples (Plymouth Marine Laboratory
301 2018, Fig. 1). In total, we identified 836 unique operational taxonomic units (OTUs),
302 attributable to 176 species within 34 orders of seaweed (Fig.1c). A higher proportion of
303 OTUs attributed to red seaweed species was always detected at the offshore site Station L4,
304 whilst the inshore sites (Firestone Bay deep and shallow, “FBD” and FBS”, respectively) had
305 a comparatively higher proportion of brown macroalgal taxa, including kelp (Fig.1a). The
306 taxonomic composition of seaweed occurring in the sedimentary eDNA pool varied
307 significantly between sites (Fig. 1b; Pseudo-F_{27,2} = 2.44, $p_{\text{perm}} < 0.01$), and between sampling
308 dates (Pseudo-F_{27,6} = 1.56, $p_{\text{perm}} < 0.05$). The latter was primarily due to a changing seaweed
309 composition of the sedimentary eDNA pool at the offshore site, over time, as previously
310 observed (Queirós et al. 2019), and there was no difference in the eDNA pools at the
311 Firestone Bay sites (Fig.1b; t (FBD/FBS) = 1.72, $p_{\text{perm}} > 0.05$). The offshore site Station L4
312 is where the highest number of OTUs was recorded throughout.

313 *Macroalgal degradation and sinking velocities*

314 Fragment sinking velocity changed over time, between species, and was size-
315 dependent (Queirós and Pascoe 2020
316) (Fig.2). All *H. elongata* fragments, of all sizes, completely degraded within 35 days. All
317 fragments of the 2 cm size group of *S. latissima*, and half of those of this size from *L. digitata*
318 and *P. palmata*, also completely degraded within 35 days. Fragments from *L. digitata*, *P.*
319 *palmata* and *S. latissima* 5 and 10 cm in length remained viable to the end of the incubations,
320 most with weights slightly increasing over time, as a potential result of fragment growth, as
321 also found by others (Frontier et al. 2021). The fragments from these three species, of all
322 sizes, were negatively buoyant at the start of the incubations, being resuspended by the action
323 of the aquarium pumps and sinking again to the bottom of the aquaria. This was also

Article

324 observed at the end of incubations. Conversely, *H. elongata* fragments were positively
325 buoyant when fresh (as recorded by others (Jones and Demetropoulos 1968)) at the start of
326 incubations, but became negatively buoyant after 6, 7 and 21 days, for fragments of 2, 5 and
327 10 cm, respectively. However, as *H. elongata* fragments degraded completely before the end
328 of the 35 day incubations, no sinking velocities were estimated for this species. For the other
329 three species, sinking velocity changed over time, between species, and with fragment size
330 (Fig.2; $\log_{10}(\text{sinking velocity}) \sim \text{date} + \text{species} + \text{fragment length} + \text{date} \times \text{species} + \text{species}$
331 $\times \text{fragment length}$; $R^2 = 56.78\%$. $F_{50,8} = 10.53$, $p < 0.01$). Fragment length generally decreased
332 sinking rates ($\beta = -0.02$, $p < 0.01$), but the reverse was true for *P. palmata* (Fig. 2, $\beta = 0.05$,
333 $p < 0.01$). The pattern of velocities was different at the start and end of incubations, but
334 changes differed among species, with a sharper decrease in velocity for *P. palmata* over time
335 than for other species (Fig.2). Potential differences between species in how mechanical
336 properties of fragments may have changed over time may thus have been important. The
337 overall mean sinking velocity over these three species, over the tested fragment size, was
338 estimated at $1.98 \pm 0.78 \text{ cm.s}^{-1}$ (mean \pm standard deviation).

339 ***Tracking trajectories of macroalgal detritus using Lagrangian particle tracking***

340 Experimentally derived mean sinking seaweed fragment velocities were used to interpret the
341 results from the particle tracking modelling. Based on these, 1D GOTM simulations (Fig. 3)
342 indicate that initially negatively buoyant seaweed detritus (e.g. *L. digitata*, *P. palmata* and *S.*
343 *latissima*) would sink and reach the seabed for the first time within one hour (Fig.3b), and
344 thus very likely near their source seaweed community around the Plymouth shore. The effect
345 of turbulent mixing in the water column results in a spread of sinking times, but this is
346 generally small (of the order of minutes, Fig. 3b). However, for buoyant seaweed detritus
347 (e.g. *H. elongata*), initial transport along the surface of the water column could allow them to
348 quickly reach waters further along the shore, or offshore, before sinking to the seabed for the

Article

349 first time (Fig. 4). Based on our experimentally-derived estimates for the time taken for *H.*
350 *elongata* fragments to become negatively buoyant (i.e. 6-21 days), our Lagrangian modeling
351 suggests that initial transport in the water column would take detritus 10-20 km along the
352 coastline and offshore before sinking to the seabed for the first time (Fig. 4). However, the
353 net direction of this transport and the proportion of detritus retained inshore before reaching
354 the seabed was strongly dependent on the release site and environmental conditions
355 experienced during that period. Specifically, in simulations starting in early May (Fig.4a, c),
356 when winds were mainly from the south-west and west (Appendix S1: Figure S7), particles
357 initially tracked east, inshore, from both sites. However, this motion was reversed after two
358 days when the wind weakened and switched to come mainly from the east. Following this
359 period, and with the switch from neap to spring tides, particles then tracked west near the
360 coast. After a week, there was a clear accumulation in Whitsand Bay for particles released
361 from both Plymouth Sound and Rame Head (Fig. 4a, c), and the particles continued to track
362 west out of the domain. In contrast, particles released during neap tides later in May rapidly
363 track east and south-east (Fig. 4b, d), moving out of the domain after a few days. In both sets
364 of simulations, a fraction of the particles released inside Plymouth Sound became trapped,
365 with some remaining within Firestone Bay (where the inshore sites we sampled are located)
366 for several days. This trapping of particles may be partially explained though the simulation
367 of particle beaching and resuspension events in the intertidal zone, slowing the passage of
368 particles out of Plymouth Sound. For the particle releases in early May, from both release
369 sites, very limited connectivity with Station L4 was observed (the offshore eDNA sampling
370 site, Fig.4a, c). In contrast, for particles released in mid to late May when the wind was
371 predominantly blowing from the south-west and west (Fig. 4b, d), stronger connectivity with
372 the offshore L4 station was estimated. This was true for particles released from both sites.
373 Indeed, during this period of strong winds from the south-west and west, and spring tides,

Article

374 lead particles reached Station L4 in just 1-2 days, and by 6 days (the shortest amount of time
375 taken for *H.elongata* fragments to become negatively buoyant during experiments) more than
376 10% of the particles had passed over the site in single releases (Fig.5a-b). Under these
377 conditions, L4 became a potential sinking site for seaweed detritus released from both sites,
378 whilst under tidal and wind patterns experienced earlier in the month, this was unlikely. The
379 impact of the wind on particle transport is consistent with the findings of (Uncles et al. 2020)
380 where the relative effect of the wind and the tide on sediment transport in the same area was
381 investigated. Seaweed detritus staying buoyant for 21 days (the longest period observed for
382 *H. elongata* fragments, during experiments) had moved outside of the modelled domain (not
383 shown) under the conditions investigated.

384 Discussion

385 The presence of macroalgal detritus within sediments (indicated via eDNA sampling) was
386 ubiquitous across our study region. Indeed, seaweed detritus was found within sediments
387 located at the inshore and offshore sites, inside and outside vegetated habitats. Our modelling
388 simulations, and our experimental assessments, suggested that, for some seaweed species, a
389 portion of detritus which is negatively buoyant upon release may be accessible to the seabed
390 very close to source. That from other species (such as *H. elongata*), being initially buoyant,
391 may reach significant distances before reaching the seabed for the first time. These
392 differences between species indicate that in the wild, where seaweed communities are
393 composed of many species, detritus should be expected to exhibit different transport
394 pathways (horizontally and vertically) across the water column, reflecting its source and
395 physical properties. As detritus degrades over time, changing in size and buoyancy, so should
396 sinking velocities be expected to change, with path complexity increasing over time, and
397 driven also by local hydrodynamics. Here, we explored the effects of tides and wind patterns
398 specifically on the connectivity between detritus source population and the seabed, but it is

Article

399 likely that other sources of environmental variability will play a key part in determining the
400 exact transport pathways. This will, in turn, depend on the specific detritus production
401 ecology of each species population(Queirós et al. 2019). Studies such as this one, including
402 observational, experimental and modelling data can help understand net detritus transport
403 pathways, and in future, inform potential hotspots for seaweed detritus accumulation. What is
404 clear, is that sedimentary sinks for this detritus are likely located not just in the deep ocean,
405 but also in the coastal ocean.

406 eDNA from species producing initially negatively buoyant detritus was found in inshore as
407 well as offshore sediments. This indicates that at least part of this detritus that reaches the
408 seabed for the first time very close to source, will become resuspended and travel further
409 offshore in subsequent events of deposition and resuspension (i.e. “saltation”), just as we
410 observed during experiments, when the water housing seaweed fragments was agitated by
411 aquarium pumps (cf. stationary conditions during which sinking velocities were measured).

412 Seaweed detritus taxonomic composition in inshore environments thus likely reflects more
413 closely that of local species, with predominantly negatively buoyant detritus upon release,
414 whilst detritus reaching the seabed further offshore will likely originate from both groups of
415 species. This was corroborated by a lower taxonomic diversity and greater similarity of
416 seaweed eDNA found in inshore sediments than that found in offshore sediments, with the
417 later potentially reflecting the ecology and release dynamics of seaweed populations from a
418 comparatively larger source pool, as previously suggested(Queirós et al. 2019).

419 Furthermore, pathways leading to carbon sequestration into the seabed compartment will be
420 affected by the specific biogeochemical properties of each sedimentary site, varying in space
421 and time(Bianchi et al. 2018; Snelgrove et al. 2018; Queirós et al. 2019). Identifying the
422 location of the seabed sinks of seaweed particulate organic carbon (released as detritus)
423 could invaluablely aid the design of management activities aiming to protect blue carbon

Article

424 habitats from disturbance, and thus support climate change mitigation(Mcleod et al. 2011;
425 Herr, Pidgeon, and Laffoley 2012). Given the findings presented in this study, the
426 identification of those sites should thus require careful consideration of a number of
427 processes. Specifically: local and regional-scaled hydrodynamic conditions; regional seaweed
428 species composition and detritus release ecology; as well as the spatial and temporal
429 dynamics of biogeochemical processes affecting seabed carbon fluxes at identified
430 sedimentary sites. As all of these properties are strongly modified by climate change driven
431 alteration of the marine ecosystems(Bianchi et al. 2021; Smale and Vance 2015; Ravaglioli et
432 al. 2019) , protecting sedimentary sinks of seaweed particulate organic carbon will also
433 require the identification of sites where carbon sequestration processes are climate-resilient or
434 increasing over time(Queirós et al. 2021).

435 *Protecting sedimentary sinks of seaweed blue carbon*

436 The three lines of evidence explored here jointly suggest that particulate seaweed detritus
437 may be broadly available for uptake in coastal sediments, where the largest proportion of
438 macroalgal production is also expected to remain(Krause-Jensen and Duarte 2016). If this is
439 also true in other coastal regions near macroalgae beds (potentially, 28% of shores
440 globally(Feehan, Filbee-Dexter, and Wernberg 2021)), and given the high productivity of
441 seaweed, then it is possible that macroalgae may drive a much larger blue carbon capability
442 than that traditionally recognized by global carbon models or protected by blue carbon
443 policies around the world, currently focused on wetlands(Sutton-Grier and Howard 2018)
444 (Fig.6). Research in our study region contemporary to the present study demonstrated that the
445 presence and taxonomic composition of seaweed eDNA in sediments reflected the ecology of
446 seaweed detritus from the surrounding shores, which in turn was reflected in the proportion
447 of seaweed carbon contributing to sedimentary carbon pools over the year(Queirós et al.
448 2019). The ubiquitous presence of seaweed eDNA within sediments in the broader region

Article

449 studied here, both inshore and offshore, suggests that sequestration of seaweed organic
450 carbon into sediments, whilst potentially peaking in specific periods of the year(Queirós et al.
451 2019), may remain within sediments beyond the seasonal cycle. And while long-term organic
452 carbon sequestration is unlikely to occur in the most dynamic areas of the coastal ocean, the
453 conditions necessary for net carbon sequestration are found across many coastal and ocean
454 shelf soft-sediment habitats(Gattuso, Frankignoulle, and Wollast 1998; Widdicombe and
455 Somerfield 2012) (e.g. fjords(Smeaton et al. 2017), muddy seabed). Furthermore, long travel
456 periods across the water column, from the shore to the deep ocean, reduce the organic carbon
457 loading of particulate detritus(Bianchi et al. 2018). These aspects challenge the often held
458 view that organic carbon sequestration may be limited to the deep sea in the open
459 ocean(Krause-Jensen and Duarte 2016), or to wetland habitats(Sutton-Grier and Howard
460 2018). Indeed, particulate organic carbon (POC) sequestration hotspots occur also elsewhere,
461 wherever high net deposition of organic material, high burial rates, low bed shear and scarcity
462 of biogeochemical oxidants (such as oxygen) are observed near and within the
463 seabed(Krause-Jensen and Duarte 2016). What's more, it is known that POC sequestration
464 hotspots are globally concentrated in soft sediments on the ocean's coastal margin, outside of
465 vegetated habitats(Krause-Jensen and Duarte 2016). And as shown here, the pathways
466 connecting seaweed particulate detritus to the seabed appear to be highly dynamic and to also
467 include coastal sediment areas, inside and outside vegetated habitats. Together with the
468 published evidence basis, our findings suggest that coastal and shelf macroalgal organic
469 carbon sinks likely exist. Further field verification of carbon fluxes at sites identified using
470 the methodologies employed here is now needed. Protecting those potential sinks, along with
471 their sources, could therefore become a viable strategy to expand the proportion of global
472 ocean falling under blue carbon activities in the near future (Fig.6)(Kuwae and Crooks 2021;
473 Queirós et al. 2019).

Article

474 Recent research has suggested protection of vast areas of the ocean toward the conservation
475 of blue carbon may be needed. But verification of realized carbon fluxes (and those of other
476 greenhouse gases) and/or an estimation of avoided emissions are a necessary steps of blue
477 carbon policy implementation(Needelman et al. 2018). As verification will be highly
478 challenging in the deep sea, as will be the enforcement of protection of sites in areas beyond
479 national jurisdiction (ABNJ), investing in the protection of those sites will likely bring
480 uncertain climate change mitigation value. In turn, the ocean's coast and shelf are where the
481 world's marine protected areas (MPAs) are already concentrated(UNEP-WCMC and IUCN
482 2020). Understanding the potential macroalgae carbon sequestration value of already
483 designated sites within national waters, or seeking the conservation of additional coastal and
484 shelf sites potentially identified in the future (as suggested here) as blue carbon activities,
485 could thus present a comparatively more certain and easier route to enhance the ocean's role
486 as a carbon sink. Supported by the type of science presented here, and with further field
487 verification of carbon flows, the current ambition to extend the world's protected areas to
488 30% of the ocean by 2030(CBD 2010) could provide the correct impetus to deliver nature-
489 based solution helping to mitigate climate-change(Austin et al. 2021). The pace of climate
490 change justifies this action(IPCC 2019, 2021). However, field measurements of the
491 ecosystem processes that drive carbon flows across ecosystems (seaweed particulate and
492 dissolved organic carbon production, POC and DOC); net sedimentary uptake (dissolved
493 inorganic production and POC uptake); carbon dating studies; and crucially, carbon source
494 partitioning studies (e.g. bulk and compound specific stable isotope analyses)(Queirós et al.
495 2019) remain rare heretofore.

496 Verifying these processes with field measurements of flows at sources and sedimentary sinks
497 could provide a necessary evidence basis to support a policy development boost toward the
498 conservation of macroalgal carbon donor and sink habitats, including natural communities as

Article

499 well as farmed seaweed(Kuwae and Crooks 2021) (Fig.6). Protecting and enhancing sources
500 and sinks together, alongside a potentially booming global seaweed farming industry, could
501 provide, in tandem, important outcomes for blue growth. Whilst protecting macroalgal carbon
502 donor and sink habitats contributes to United Nations Sustainable Development Goals 13 and
503 14(United Nations 2015) (“SDG”, limit climate change and protect life under water,
504 respectively), an informed expansion of the seaweed industry could be harnessed in this way
505 too, helping to deliver on those aims, as well as further supporting the delivery of SDG2 and
506 5 (alleviate poverty, gender equality, respectively)(United Nations 2015). For instance, in the
507 Western Indian Ocean region, seaweed farming is a socially valuable activity because it is
508 primarily undertaken by women, and their key livelihood(Msuya 2012).

509 The importance of capturing ecosystem connectivity within Marine Protected Areas and other
510 effective area-based conservation measures’ design has been previously recognized for other
511 purposes(Carr et al. 2017). Capturing also the connectivity of macroalgae organic carbon
512 donors and sinks within such mechanisms could potentially greatly expand the global ocean’s
513 blue carbon capability harnessed within conservation areas(Queirós et al. 2019). Further field
514 verification of macroalgae detritus transport pathways elucidated via modelling shown here,
515 and a close collaboration with practitioners, may help to guide the development of the next
516 stage of blue carbon research. This should now seek to provide policy makers with needed,
517 field-based carbon flow rate measurements (and of their variability) for spatially explicit
518 carbon sources and sinks. Such evidence would allow for much needed, improved ocean
519 carbon accounting, which should in turn be used to inform the design of future-proofed, and
520 actionable, blue carbon conservation mechanisms.

521

522 *The next frontiers in macroalgal blue carbon research supporting conservation*

Article

523 A recent field data provided evidence that macroalgal detritus can travel a substantial
524 distance from source locations³¹. The data presented here supports this view, suggesting that,
525 in a given site, macroalgal beds contributing to a detritus pool available to sediments may be
526 located both local and at far-afield locations. Differences in the sedimentary eDNA pools
527 analysed here, varying over time and space, indicated potentially different dynamics of
528 detrital connectivity and transport from sources to sediments. To our knowledge, this is the
529 first study employing Lagrangian particle-tracking in this context. We illustrated the
530 importance of environmental conditions, and their effects on hydrodynamic patterns, in
531 establishing connectivity routes between seaweed communities exporting detritus to different
532 areas of the seabed. However, longer model simulations, the inclusion of missing processes
533 such as saltation, Stoke's drift, and the refinement of simulated particle properties to better
534 reflect observed changes in seaweed detritus attributes over time, will be required to identify
535 long-term, macroalgal detritus accumulation sites. Other processes still, about which we
536 know very little, will further affect these transport pathways, including: the detritus release
537 ecology of source species; the mechanical properties of the released detritus (e.g. autumn,
538 wave-driven whole detachment cf. loss of small, degraded fragments over time); and the
539 balance between fragment viability during transport and degradation(Queirós et al. 2019;
540 Frontier et al. 2021). As recently found by others(Frontier et al. 2021), our experiments also
541 suggest that macroalgal fragments may remain viable for long periods after export from their
542 source. This, in turn, may extend transport time and support long travel distances for
543 macroalgal fragments(Filbee-Dexter et al. 2018).

544 The use of eDNA as evidence of the presence of a macroalgal signature within sea-bed
545 habitats is growing. It is unarguably an invaluable tool to track the transfer of macroalgal
546 detritus from shore to seabed, and can offer a more detailed taxonomic discrimination of taxa
547 present than other techniques. This provides important evidence that helps understand the

Article

548 ecological processes underpinning macroalgal blue carbon(Ortega, Geraldi, and Duarte 2020;
549 Queirós et al. 2019). However, given the spatial and temporal contextual specificity of the
550 seabed processes that determine carbon sequestration rates(Queirós et al. 2019; Legge et al.
551 2020; Snelgrove et al. 2018), and the dynamic nature of transport pathways connecting
552 macroalgal beds to potential sedimentary carbon sinks sites, it seems ill-advised to expect that
553 any site specific relationship between sedimentary macroalgal eDNA and POC stores should
554 be expected to hold ubiquitously(Ortega et al. 2019; Anglès d'Auriac et al. 2021).

555 Linking macroalgal carbon sources and sinks is, at least in part, a biotracing problem, and
556 biotracing in natural ecosystems typically requires more than one technique to be employed,
557 given the uncertainties of each approach(Nielsen et al. 2018). For instance, using a
558 combination of Bayesian stable isotope mixing modelling and seabed process measurements,
559 a previous study established that macroalgal eDNA in sediments at our offshore site appeared
560 to reflect the seasonal ecology of both source populations and the seabed habitat(Queirós et
561 al. 2019). And as with any technique, it must be acknowledged that a suite of validation and
562 optimization experiments are also necessary to fully exploit the usefulness of eDNA in such
563 environmental studies, now and into the future. For instance, and as done here, sample
564 collection and preparation must be optimized (*e.g.* sediment volumes and choice of DNA
565 extraction methods specifically designed for difficult to lyse seaweed fragments). Secondly,
566 the choice and design of PCR primers should always be scrutinized. Because macroalgal blue
567 carbon science is in its infancy, in the present study, as in others(Ortega et al. 2019; Ortega,
568 Geraldi, and Duarte 2020), universal 18S rRNA PCR primers that amplify short (~260 bp)
569 DNA fragments have been used to enable the detection of as wide a range of macroalgal taxa
570 as possible, but these offer limited taxonomic resolution for some taxa. Advances in DNA
571 sequencing technology that enable sequencing of longer DNA fragments will provide more
572 detailed identification(Anglès d'Auriac et al. 2021). Together with the population of public

Article

573 DNA databases with sequences of as many taxa as possible, the accuracy of taxonomic
574 identification via eDNA studies will also increase(Queirós et al. 2019). Thirdly, and crucially,
575 the potential use of eDNA to assess the prevalence and diversity of macroalgae detritus
576 within sediments requires robust understanding of the persistence of eDNA, and the factors
577 controlling macroalgal detritus degradation and eDNA decomposition, both of which we are
578 only beginning to investigate as a community. Combining eDNA analysis with other
579 approaches, such as carbon sequestration rate measurements and carbon source partitioning
580 via stable isotope techniques, is thus likely to provide a more robust evidence basis necessary
581 to inform the potential need to develop macroalgal blue carbon activities. For these reasons
582 we should not, and cannot, build better carbon accounting or improve global biogeochemical
583 modelling based on eDNA data alone. Finally, the argument for conserving macroalgal
584 carbon sequestration sites (Fig.6) requires us to think about long-term sequestration, and thus
585 also about the sensitivity of these sites and carbon flows to climate change(Ravaglioli et al.
586 2019). Investing in blue carbon conservation without acknowledging these effects is thus
587 unlikely to produce tangible climate change mitigation. This too requires further work.

588

589 Acknowledgements

590 AMQ, KT and PJS acknowledge funding from the UK Natural Environment Research
591 Council (NERC) and Department for Environment, Food and Rural Affairs, Marine
592 Ecosystems Research Programme (# NE/L00299X/1). AMQ and PJS further acknowledge
593 funding from the European Union's Horizon 2020 FutureMARES project (#869300). KT
594 acknowledges funding from the NERC MARINE-DNA project (#NE/N006100/1). DS is
595 supported by a UKRI Future Leaders Fellowship (MR/S032827/1). PJS and JC acknowledge
596 funding support from the NERC through its National Capability Long-term Single Centre
597 Science Programme, Climate Linked Atlantic Sector Science (#NE/R015953/1). RT and MB

Article

598 acknowledge support by the European Union's Interreg Atlantic Area project MyCOAST
599 (#EAPA_285/2016).

600

PRE-PRINT

Article

601 **References**

- 602 Amaral-Zettler, Linda A, Elizabeth A McCliment, Hugh W Ducklow, and Susan M Huse.
603 2009. 'A method for studying protistan diversity using massively parallel sequencing
604 of V9 hypervariable regions of small-subunit ribosomal RNA genes', *PloS one*, 4:
605 e6372.
- 606 Anderson, Marti J. 2014. 'Permutational multivariate analysis of variance (PERMANOVA)',
607 *Wiley statsref: statistics reference online*: 1-15.
- 608 Anglès d'Auriac, Marc, Kasper Hancke, Hege Gundersen, Helene Frigstad, and Gunhild
609 Borgersen. 2021. 'Blue Carbon eDNA—A novel eDNA method to trace macroalgae
610 carbon in marine sediments', *NIVA-rapport*.
- 611 Austin, W., F. Cohen, D. Coomes, N. Hanley, S. Lewis, R. Luque-Lora, R. Marchant, L.
612 Naylor, A. M. Queirós, A. Savaresi, N. Seddon, A. Smith, P. Smith, and C. Wheeler.
613 2021. "Nature-based solutions for climate change, people and biodiversity." In
614 *COP26 Universities Network Briefing*.
- 615 Bianchi, Thomas S, Robert C Aller, Trisha B Atwood, Craig J Brown, Luis A Buatois, Lisa A
616 Levin, Jeffrey S Levinton, Jack J Middelburg, Elise S Morrison, and Pierre Regnier.
617 2021. 'What global biogeochemical consequences will marine animal–sediment
618 interactions have during climate change?', *Elem Sci Anth*, 9: 00180.
- 619 Bianchi, Thomas S, Xingqian Cui, Neal E Blair, David J Burdige, Timothy I Eglinton, and
620 Valier Galy. 2018. 'Centers of organic carbon burial and oxidation at the land-ocean
621 interface', *Organic Geochemistry*, 115: 138-55.
- 622 Carr, Mark H, Sarah P Robinson, Charles Wahle, Gary Davis, Stephen Kroll, Samantha
623 Murray, Ervin Joe Schumacker, and Margaret Williams. 2017. 'The central
624 importance of ecological spatial connectivity to effective coastal marine protected

Article

- 625 areas and to meeting the challenges of climate change in the marine environment',
626 *Aquatic Conservation: Marine and Freshwater Ecosystems*, 27: 6-29.
- 627 CBD. 2010. 'Report of the Tenth Meeting of the Conference of the Parties to the Convention
628 on Biological Diversity'.
- 629 Chen, Changsheng, Hedong Liu, and Robert C Beardsley. 2003. 'An unstructured grid, finite-
630 volume, three-dimensional, primitive equations ocean model: application to coastal
631 ocean and estuaries', *Journal of atmospheric and oceanic technology*, 20: 159-86.
- 632 De Leij, Rebecca, Graham Epstein, Matthew P Brown, and Dan A Smale. 2017. 'The
633 influence of native macroalgal canopies on the distribution and abundance of the non-
634 native kelp *Undaria pinnatifida* in natural reef habitats', *Marine Biology*, 164: 1-15.
- 635 Feehan, Colette J, Karen Filbee-Dexter, and Thomas Wernberg. 2021. 'Embrace kelp forests
636 in the coming decade', *Science*, 373: 863-63.
- 637 Filbee-Dexter, Karen, Thomas Wernberg, Kjell Magnus Norderhaug, Eva Ramirez-Llodra,
638 and Morten Foldager Pedersen. 2018. 'Movement of pulsed resource subsidies from
639 kelp forests to deep fjords.', *Oecologia*, 187: 291-304.
- 640 Friedlingstein, Pierre, Michael O'sullivan, Matthew W Jones, Robbie M Andrew, Judith
641 Hauck, Are Olsen, Glen P Peters, Wouter Peters, Julia Pongratz, and Stephen Sitch.
642 2020. 'Global carbon budget 2020', *Earth System Science Data*, 12: 3269-340.
- 643 Frontier, Nadia, Florian de Bettignies, Andy Foggo, and Dominique Davoult. 2021.
644 'Sustained productivity and respiration of degrading kelp detritus in the shallow
645 benthos: Detached or broken, but not dead', *Marine Environmental Research*, 166:
646 105277.
- 647 Gallo, Natalya D, David G Victor, and Lisa A Levin. 2017. 'Ocean commitments under the
648 Paris Agreement', *Nature Climate Change*, 7: 833.

Article

- 649 Gattuso, J-P, M Frankignoulle, and R Wollast. 1998. 'Carbon and carbonate metabolism in
650 coastal aquatic ecosystems', *Annual Review of Ecology and Systematics*: 405-34.
- 651 Herr, D. , E. Pidgeon, and D Laffoley. 2012. "Blue Carbon Policy Framework: Based on the
652 discussion of the International Blue Carbon Policy Working Group." In, vi+39pp.
653 Gland, Switzerland: IUCN and Arlington, USA: CI.
- 654 Hoegh-Guldberg, Ove, Ken Caldeira, Thierry Chopin, Steve Gaines, Peter Haugan, Mark
655 Hemer, Jennifer Howard, Manaswita Konar, Dorte Krause-Jensen, Elizabeth
656 Lindstad, Catherine E. Lovelock, Mark Michelin, Finn Gunnar Nielsen, Eliza
657 Northrop, Robert Parker, Joyashree Roy, Tristan Smith, Shreya Some, and Peter
658 Tyedmers. 2019. "The Ocean as a Solution to Climate Change: Five Opportunities for
659 Action." In, edited by Ove Hoegh-Guldberg, 111. Washington, DC: World Resources
660 Institute.
- 661 Hunt, OD. 1925. 'The food of the bottom fauna of the Plymouth fishing grounds', *Journal of*
662 *the Marine Biological association of the United Kingdom*, 13: 560-99.
- 663 IPCC. 2019. "IPCC Special Report on the Ocean and Cryosphere in a Changing Climate." In,
664 edited by H.-O. Pörtner, D.C. Roberts, V. Masson-Delmotte, P. Zhai, M. Tignor, E.
665 Poloczanska, K. Mintenbeck, A. Alegría, M. Nicolai, A. Okem, J. Petzold, B. Rama
666 and N.M. Weyer, in press. IPCC.
- 667 ———. 2021. "Climate Change 2021 - The Physical Science Basis. Working Group I
668 contribution to the Sixth Assessment Report of the Intergovernmental Panel on
669 Climate Change." In.
- 670 Jones, W Eifion, and Andreas Demetropoulos. 1968. 'Exposure to wave action:
671 measurements of an important ecological parameter on rocky shores on Anglesey',
672 *Journal of Experimental Marine Biology and Ecology*, 2: 46-63.

Article

- 673 Krause-Jensen, Dorte, and Carlos M. Duarte. 2016. 'Substantial role of macroalgae in marine
674 carbon sequestration', *Nature Geoscience*, 9: 737–42
- 675 Krause-Jensen, Dorte, Paul Lavery, Oscar Serrano, Núria Marba, Pere Masque, and Carlos M
676 Duarte. 2018. 'Sequestration of macroalgal carbon: the elephant in the Blue Carbon
677 room', *Biology letters*, 14: 20180236.
- 678 Kuwae, Tomohiro, and Stephen Crooks. 2021. 'Linking climate change mitigation and
679 adaptation through coastal green–gray infrastructure: a perspective', *Coastal
680 Engineering Journal*: 1-12.
- 681 Kuwae, Tomohiro, Atsushi Watanabe, Satoru Yoshihara, Fujiyo Suehiro, and Yoshihisa
682 Sugimura. 2022. 'Implementation of blue carbon offset crediting for seagrass
683 meadows, macroalgal beds, and macroalgae farming in Japan', *Marine Policy*, 138:
684 104996.
- 685 Legge, Oliver, Martin Johnson, Natalie Hicks, Tim Jickells, Markus Diesing, John Aldridge,
686 Julian Andrews, Yuri Artioli, Dorothee Bakker, Michael Burrows, Nealy Carr,
687 Gemma Cripps, Stacey Felgate, Liam Fernand, Naomi Greenwood, Susan Hartman,
688 Silke Kröger, Gennadi Lessin, Claire Mahaffey, Daniel Mayor, Ruth Parker, Ana
689 Queiros, Jamie Shutler, Tiago Silva, Henrik Stahl, Jonathan Tinker, Graham
690 Underwood, Johan Van Der Molen, Sarah Wakelin, Keith Weston, and Phillip
691 Williamson. 2020. 'Carbon on the Northwest European Shelf: Contemporary Budget
692 and Future Influences', *Frontiers in Marine Science*.
- 693 Li, Hongmei, Zenghu Zhang, Tianqi Xiong, Kunxian Tang, Chen He, Quan Shi, Nianzhi
694 Jiao, and Yongyu Zhang. 2022. 'Carbon Sequestration in the Form of Recalcitrant
695 Dissolved Organic Carbon in a Seaweed (Kelp) Farming Environment',
696 *Environmental Science & Technology*.

Article

- 697 Mcleod, Elizabeth, Gail L Chmura, Steven Bouillon, Rodney Salm, Mats Björk, Carlos M
698 Duarte, Catherine E Lovelock, William H Schlesinger, and Brian R Silliman. 2011. 'A
699 blueprint for blue carbon: toward an improved understanding of the role of vegetated
700 coastal habitats in sequestering CO₂', *Frontiers in Ecology and the Environment*, 9:
701 552-60.
- 702 Msuya, Flower E. 2012. 'A study of working conditions in the Zanzibar seaweed farming
703 industry', *Women in Informal Employment: Globalizing and organizing (WIEGO)*,
704 *Cambridge, MA*.
- 705 Needelman, Brian A, Iginio M Emmer, Stephen Emmett-Mattox, Stephen Crooks, J Patrick
706 Megonigal, Doug Myers, Matthew PJ Oreska, and Karen McGlathery. 2018. 'The
707 science and policy of the verified carbon standard methodology for tidal wetland and
708 seagrass restoration', *Estuaries and Coasts*, 41: 2159-71.
- 709 Nielsen, Jens M, Elizabeth L Clare, Brian Hayden, Michael T Brett, and Pavel Kratina. 2018.
710 'Diet tracing in ecology: method comparison and selection', *Methods in Ecology and*
711 *Evolution*, 9: 278-91.
- 712 North West Shelf Monitoring and Forecasting Center. 2020. "Ocean biogeochemistry
713 reanalysis for the North-West European Shelf, E.U. Copernicus Marine Service
714 Information. [https://resources.marine.copernicus.eu/product-](https://resources.marine.copernicus.eu/product-detail/NWSHELF_MULTIYEAR_BGC_004_011/INFORMATION)
715 [detail/NWSHELF_MULTIYEAR_BGC_004_011/INFORMATION](https://resources.marine.copernicus.eu/product-detail/NWSHELF_MULTIYEAR_BGC_004_011/INFORMATION)." In.
- 716 Ortega, Alejandra, Nathan R Geraldi, Intikhab Alam, Allan A Kamau, Silvia G Acinas,
717 Ramiro Logares, Josep M Gasol, Ramon Massana, Dorte Krause-Jensen, and Carlos
718 M Duarte. 2019. 'Important contribution of macroalgae to oceanic carbon
719 sequestration', *Nature Geoscience*, 12: 748-54.

Article

- 720 Ortega, Alejandra, Nathan R Geraldi, and Carlos M Duarte. 2020. 'Environmental DNA
721 identifies marine macrophyte contributions to Blue Carbon sediments', *Limnology and*
722 *Oceanography*.
- 723 Plymouth Marine Laboratory. 2018. "Eukaryote diversity assessment of sediments of the
724 Western English Channel." In. NCBI SRA.
- 725 Polis, Gary A, Wendy B Anderson, and Robert D Holt. 1997. 'Toward an integration of
726 landscape and food web ecology: The Dynamics of Spatially Subsidized Food Webs',
727 *Annu. Rev. Ecol. Syst.*, 28: 289-316.
- 728 Queirós, A. M., and C. Pascoe. 2020
- 729 "Mesocosms investigation of seaweed fragment degradation and skinking rates." In. Zenodo.
- 730 Queirós, A.M., E. Talbot, N.J. Beaumont, PJ Somerfield, S. Kay, C. Pascoe, S. Dedman, J.
731 Fernandes, A. Jütterbrock, P.I. Miller, S.F. Saille, G. Sará, L.M. Carr, M.C. Austen,
732 S. Widdicombe, G. Rilov, L.A. Levin, S.C. Hull, S.F. Walmsley, and C. Nic
733 Aonghusa. 2021. 'Bright spots as climate-smart marine spatial planning tools for
734 conservation and blue growth ', *Global Change Biology*, 27: 5514-31.
- 735 Queirós, Ana M, Nicholas Stephens, Richard Cook, Chiara Ravaglioli, Joana Nunes, Sarah
736 Dashfield, Carolyn Harris, Gavin H. Tilstone, James Fishwick, Ulrike Braeckman,
737 Paul Somerfield, and Stephen Widdicombe. 2015. 'Can benthic community structure
738 be used to predict the process of bioturbation in real ecosystems?', *Progress in*
739 *Oceanography*, 137: 559–69.
- 740 Queirós, Ana M, Nicholas Stephens, Stephen Widdicombe, Karen Tait, Sophie J McCoy,
741 Jeroen Ingels, Saskia Rühl, Ruth Airs, Amanda Beesley, Giorgia Carnovale, Pierre
742 Cazenave, Sarah Dashfield, Er Hua, Mark Jones, Penelope Lindeque, Caroline L.
743 McNeill, Joana Nunes, Helen Parry, Christine Pascoe, Claire Widdicombe, Tim
744 Smyth, Angus Atkinson, Dorte Krause-Jensen, and Paul J Somerfield. 2019.

Article

- 745 'Connected macroalgal-sediment systems: blue carbon and foodwebs in the deep
746 coastal ocean ', *Ecological Monographs*, 89: e01366.
- 747 Queirós, Ana M., José A. Fernandes, Sarah Faulwetter, Joana Nunes, Samuel P. S. Rastrick,
748 Nova Mieszkowska, Yuri Artioli, Andrew Yool, Piero Calosi, Christos Arvanitidis,
749 Helen S. Findlay, Manuel Barange, William W. L. Cheung, and Stephen
750 Widdicombe. 2015. 'Scaling up experimental ocean acidification and warming
751 research: from individuals to the ecosystem', *Global Change Biology*, 21: 130-43.
- 752 R Core Team. 2020. "R: A language and environment for statistical computing." In. Vienna,
753 Austria: R Foundation for Statistical Computing.
- 754 Ravaglioli, Chiara, Fabio Bulleri, Saskia Rühl, Sophie J. McCoy, Helen Findlay, Steven
755 Widdicombe, and Ana M. Queirós. 2019. 'Ocean acidification and hypoxia alter
756 organic carbon fluxes in marine soft sediments', *Global Change Biology*, 25: 4165-78.
- 757 Raven, John. 2018. 'Blue carbon: past, present and future, with emphasis on macroalgae',
758 *Biology letters*, 14: 20180336.
- 759 Skamarock, William C, Joseph B Klemp, Jimy Dudhia, David O Gill, Dale M Barker, Wei
760 Wang, and Jordan G Powers. 2008. 'A description of the Advanced Research WRF
761 version 3. NCAR Technical note-475+ STR'.
- 762 Smagorinsky, Joseph. 1963. 'General circulation experiments with the primitive equations: I.
763 The basic experiment', *Monthly weather review*, 91: 99-164.
- 764 Smale, DA, and T Vance. 2015. 'Climate-driven shifts in species' distributions may
765 exacerbate the impacts of storm disturbances on North-east Atlantic kelp forests',
766 *Marine and Freshwater Research*, 67: 65.
- 767 Smale, Dan A., Pippa J. Moore, Ana M Queiros, Nicholas D. Higgs, and Michael T.
768 Burrows. 2018. 'Appreciating interconnectivity between habitats is key to Blue
769 Carbon management', *Frontiers in Ecology and the Environment* 16: 71-73.

Article

- 770 Smale, Dan A., Albert Pessarrodona, Nathan King, and Pippa J. Moore. *in press*. 'Examining
771 the production, export, and immediate fate of kelp detritus on open-coast subtidal
772 reefs in the Northeast Atlantic', *Limnology and Oceanography*.
- 773 Smeaton, Craig, William EN Austin, Althea L Davies, Agnes Baltzer, John A Howe, and
774 John M Baxter. 2017. 'Scotland's forgotten carbon: a national assessment of mid-
775 latitude fjord sedimentary carbon stocks', *Biogeosciences*, 14: 5663-74.
- 776 Smith, SV. 1981. 'Marine macrophytes as a global carbon sink', *Science*, 211: 838-40.
- 777 Smyth, T, A Atkinson, S Widdicombe, M Frost, JI Allen, J Fishwick, AM Queirós, D Sims,
778 and M Barange. 2015. 'The Western Channel Observatory', *Progress in*
779 *Oceanography*, 137: 335-41.
- 780 Snelgrove, Paul VR, Karline Soetaert, Martin Solan, Simon Thrush, Chih-Lin Wei, Roberto
781 Danovaro, Robinson W Fulweiler, Hiroshi Kitazato, Baban Ingole, and Alf Norkko.
782 2018. 'Global Carbon Cycling on a Heterogeneous Seafloor', *Trends in Ecology &*
783 *Evolution*, 33: 96-105.
- 784 Sutton-Grier, Ariana, and Jennifer Howard. 2018. 'Coastal wetlands are the best marine
785 carbon sink for climate mitigation', *Frontiers in Ecology and the Environment*, 16:
786 73-74.
- 787 Umlauf, Lars, and Hans Burchard. 2005. 'Second-order turbulence closure models for
788 geophysical boundary layers. A review of recent work', *Continental Shelf Research*,
789 25: 795-827.
- 790 Uncles, RJ, JR Clark, M Bedington, and R Torres. 2020. 'On sediment dispersal in the
791 Whitsand Bay Marine Conservation Zone: Neighbour to a closed dredge-spoil
792 disposal site.' in, *Marine Protected Areas* (Elsevier).

Article

- 793 UNEP-WCMC, and IUCN. 2020. "Protected Planet: The World Database on Protected Areas
794 (WDPA) and World Database on Other Effective Area-based Conservation Measures
795 (WD-OECM) " In. www.protectedplanet.net.
- 796 United Nations. 2015. 'Transforming our world: The 2030 agenda for sustainable
797 development', *New York: United Nations, Department of Economic and Social
798 Affairs*.
- 799 Widdicombe, S., and P.J. Somerfield. 2012. 'Marine biodiversity: its past development,
800 present status, and future threats', *Marine Biodiversity and Ecosystem Functioning:
801 Frameworks, methodologies, and integration*: 1.

PRE-PRINT

Article

803 **Figure captions**

804 **Figure 1:** The composition of eDNA in sedimentary samples, from the three sampled sites:
805 the inshore sites are Firestone Bay “shallow” (“FBS”) and Firestone Bay “deep” (“FBD”);
806 the offshore site is station L4. a) Pie charts give the mean relative seaweed sequence
807 abundance per class and sampling site and time point (3-4 replicates, except for May 2016 at
808 L4, when there was only 1 replicate). Pie chart shading reflects the proportion of sedimentary
809 eDNA sequences retrieved from macroalgae classes: Compsopogonophyceae (light pink);
810 Bangiophyceae (pink); Florideophyceae (red); Phaeophyceae (brown); and Ulvophyceae
811 (green). b) similarity of sedimentary eDNA sequences for seaweed per site, with inshore sites
812 separating from the offshore site. c) seaweed taxa diversity per time point and sampled area,
813 showing that sedimentary eDNA at inshore sites corresponds to a lower number of seaweed
814 taxa than that found offshore.

815 **Figure 2:** The sinking velocity of seaweed fragments, at the start (a) and end (b) of 35 day
816 incubations.

817 **Figure 3:** 1D simulations of seaweed detritus settling out through a turbulent water column.
818 Results are generated using the particle tracking model PyLag coupled to GOTM, using a
819 configuration for Station L4 in the WEC (see Appendix S1). Diagram (a) illustrates the
820 sinking of (green) seaweed fragments over time (t). Insert plot (b) shows the estimated
821 fraction of particles remaining in the water column as a function of time, for a range of fixed
822 particle sinking velocities. The average measured sinking velocity of blade/strap fragments in
823 the laboratory was $0.019 \pm 0.008 \text{ m}\cdot\text{s}^{-1}$. In each case, 10,000 particles were released from the
824 surface of the water column at midnight on 1st May 2021. The depth of the water column is
825 50 m.

826 **Figure 4:** Simulated spatial distribution of buoyant seaweed fragments released from
827 Plymouth Sound (a, b) and Rame Head (c, d) under contrasting environmental conditions

Article

828 (please see Fig. 1 for release site location). In each case, 1000 particles are released at high
829 water from the two sites, starting at 1215 on 1st May 2016 (a, c) and 0100 on 16th May 2016
830 (b, d). A further 1000 particles are released at each subsequent high water. Particle positions
831 are plotted at 09:45 on the 8th May 2016 (a, c) and at 21:15 on 22nd May 2016 (b, d),
832 corresponding to a time three hours after high water following the 14th release of particles
833 (see also Fig. S7b). Station L4 is identified with a star.

834 **Figure 5:** Histograms showing the time taken (“time of flight”) for buoyant particles to reach
835 L4 station after release from Plymouth Sound (a) and Rame Head (b). Simulations were
836 carried out during the second half of May 2016, during a period of strong southerly winds.
837 Results are based on the full ensemble of runs (14 members, 10,000 particles released per
838 member per release site). The 14 releases were performed at consecutive high waters starting
839 at 01:00 on 16th May 2016. The time of transport is computed from the difference between
840 the release time and the first time point at which the particle is observed in the box bounding
841 the L4 benthic sampling site (SI Fig. S7a).

842 **Figure 6:** In habitats typically captured by blue carbon conservation schemes (saltmarsh,
843 seagrass meadows and mangroves), CO₂ is fixed in the same area where organic carbon is
844 sequestered (a), so that protected habitat patches deliver the whole blue carbon process (C_{org}
845 $C_{\text{org source}}$ and $C_{\text{org sink}}$). Protecting connected macroalgal-sediment blue carbon (b) requires the
846 protection of highly productive macroalgal communities where CO₂ is fixed into the living
847 biomass ($C_{\text{org source}}$) as well as the seabed hotspots of sequestration where exported
848 macroalgal organic carbon sinks ($C_{\text{org sink}}$) after transport across the coastal ocean.

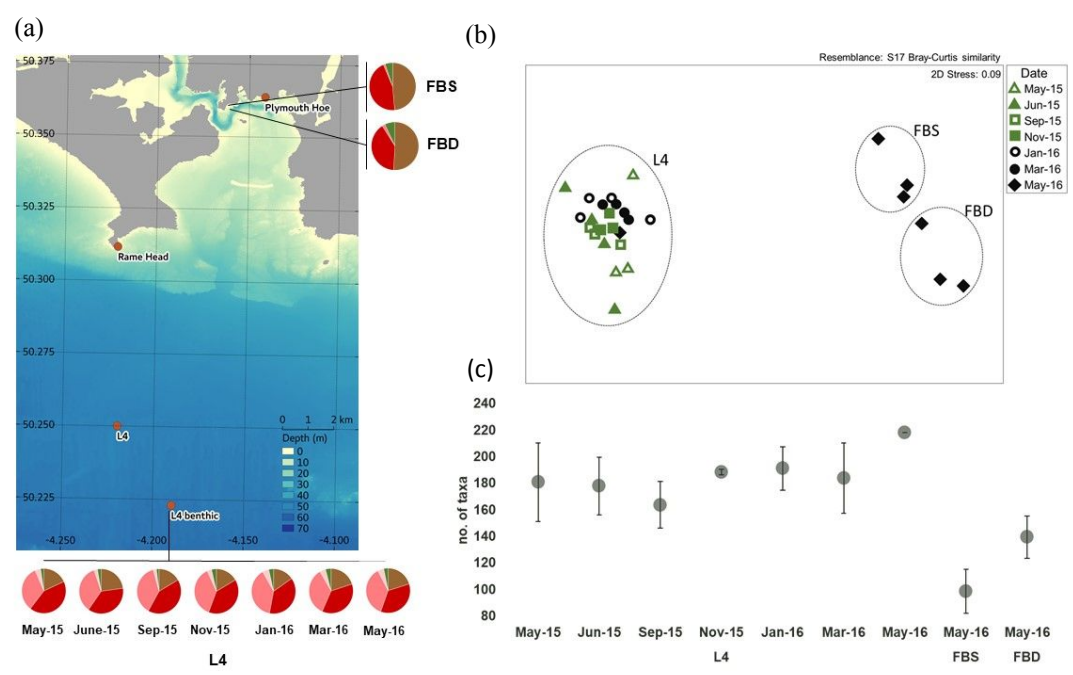
849

850

851

852

853 **Figures**

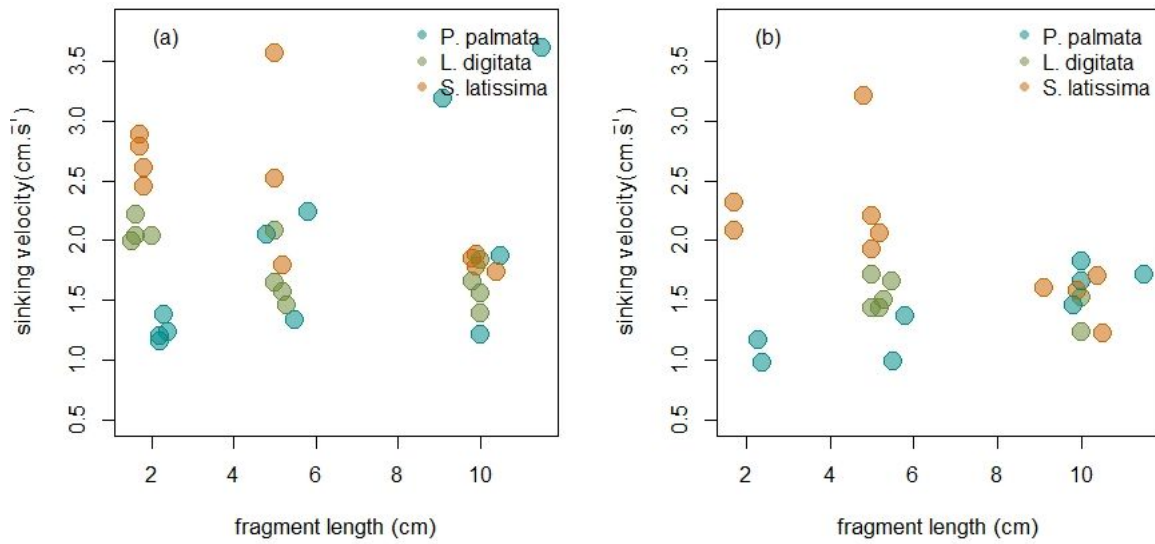


854

855 **Figure 1**

PRE-PRINT

Article



856

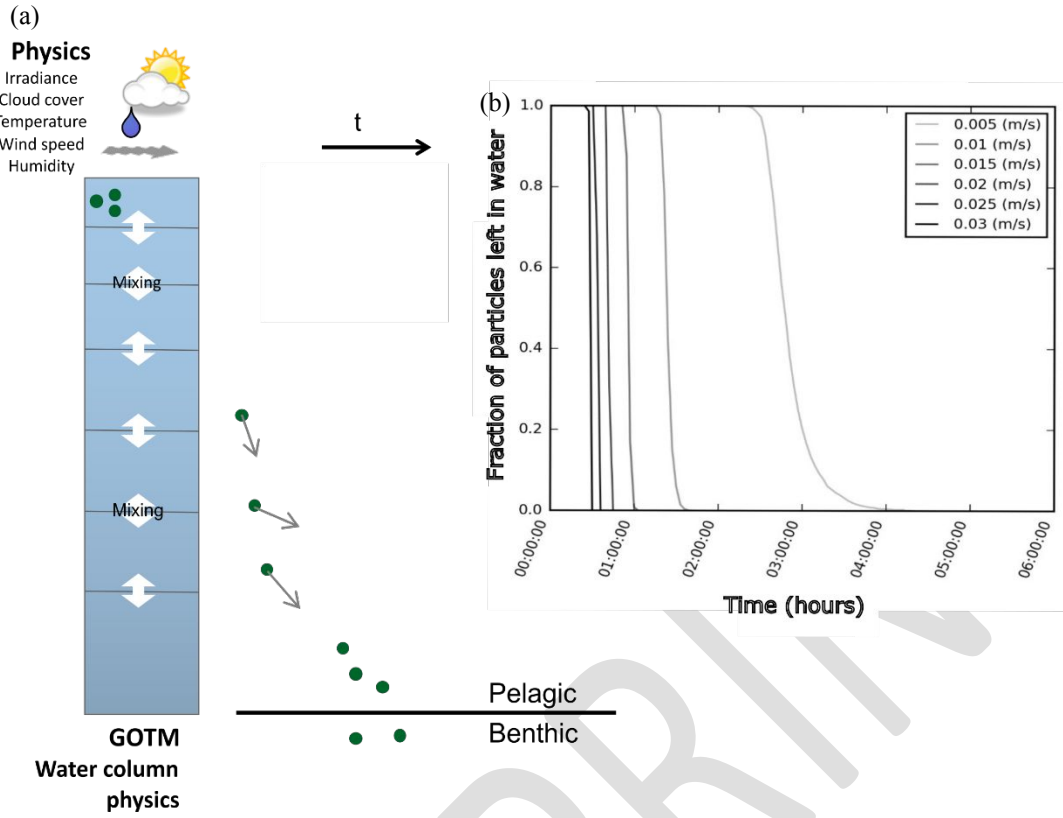
857 **Figure 2**

858

PRE-PRINT

Article

859

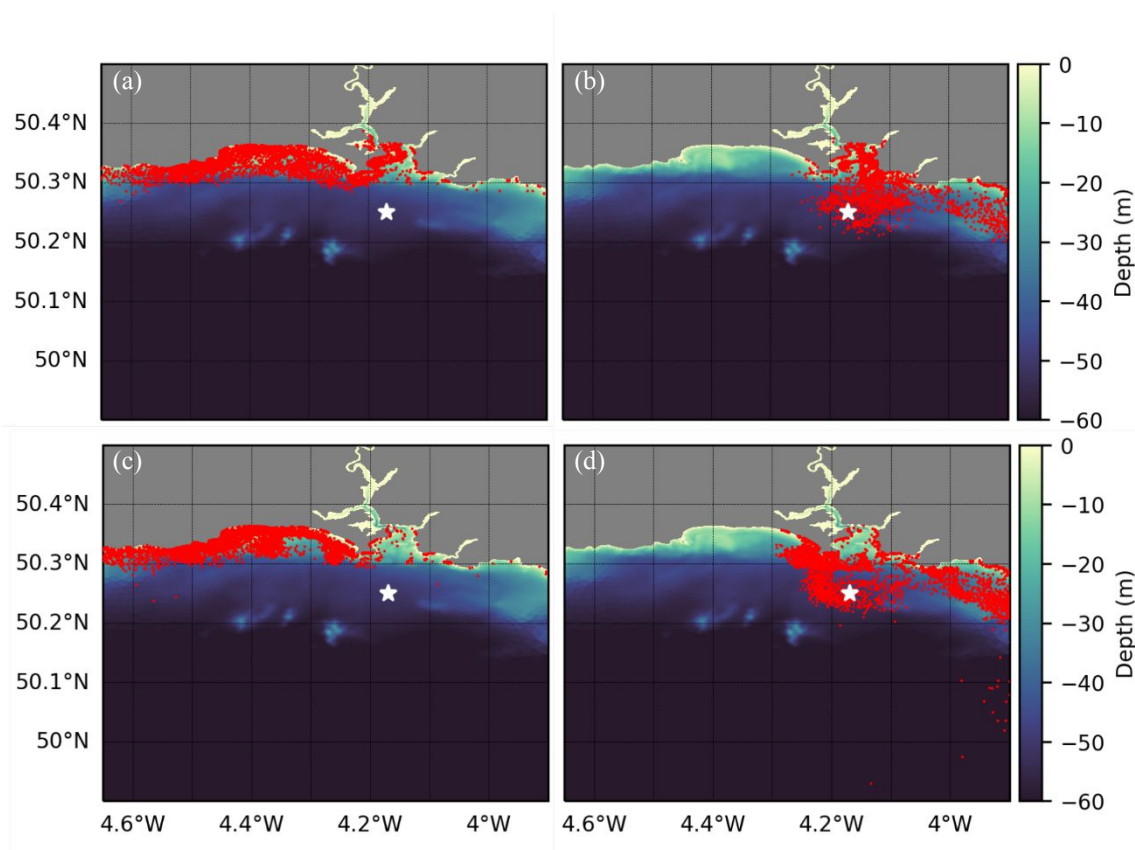


860

861 **Figure 3**

862

Article

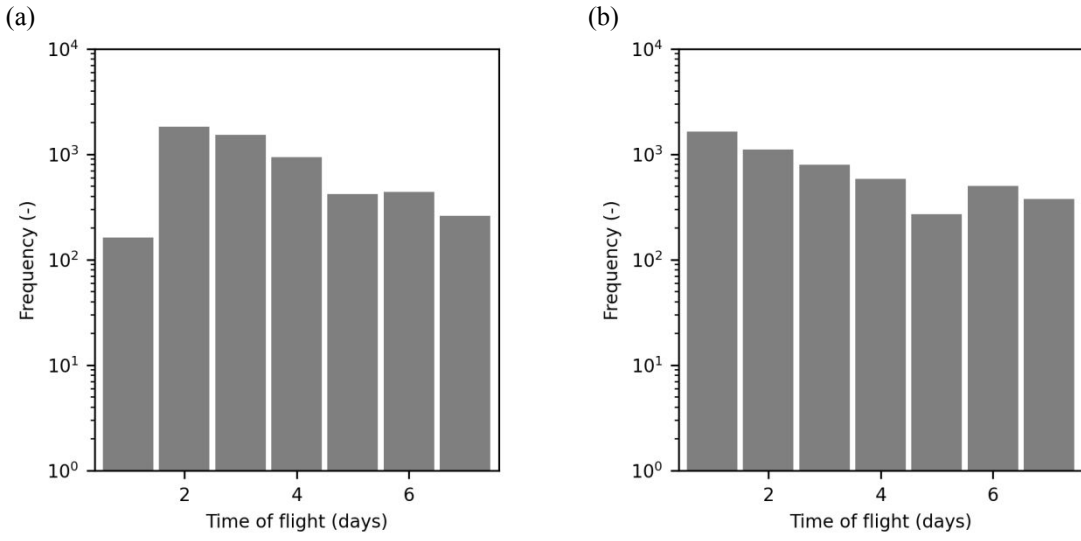


863

864 **Figure 4**

865

Article



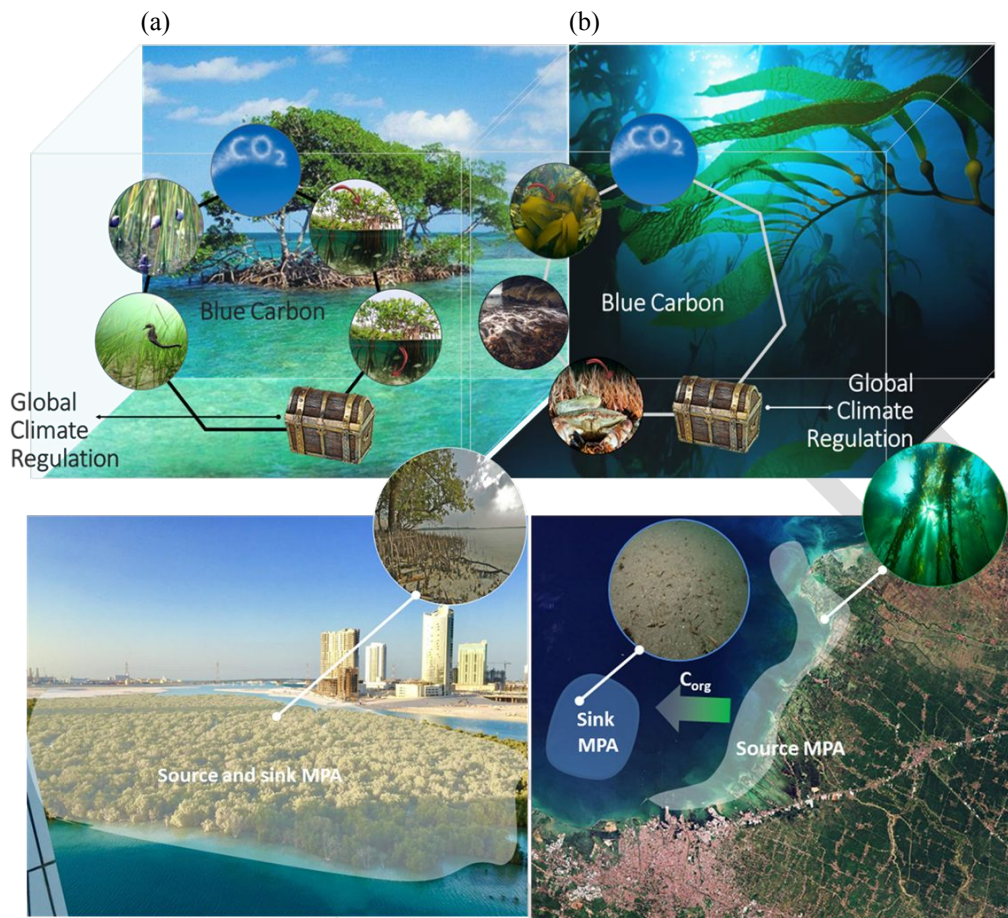
866

867 **Figure 5**

868

PRE-PRINT

869



870

871 **Figure 6**

872

873